E and M SARS-CoV-2 membrane protein expression and enrichment with plant lipid droplets

Lionel Gissot, Florent Fontaine, Zsolt Kelemen, Ousmane Dao, Isabelle Bouchez, Carine Deruyffelaere, Michèle Winkler, Anais Da Costa, Fabienne Pierre, Chouaib Meziadi, et al.

Received: 26 September 2023 | Revised: 9 November 2023 | Accepted: 13 November 2023

DOI: 10.1002/biot.202300512

Biotechnology Journal

RESEARCH ARTICLE

E and M SARS-CoV-2 membrane protein expression and enrichment with plant lipid droplets

Lionel Gissot[1] | Florent Fontaine[2] | Zsolt Kelemen[1] | Ousmane Dao[1] | Isabelle Bouchez[1] | Carine Deruyffelaere[1] | Michèle Winkler[1] | Anais Da Costa[1] | Fabienne Pierre[2] | Chouaib Meziadi[2] | Jean-Denis Faure[1] | Marine Froissard[1]

[1]Université Paris-Saclay, INRAE, AgroParisTech, Institut Jean-Pierre Bourgin (IJPB), Versailles, France

[2]SAS Core Biogenesis, 850 Bd Sébastien Brant BioParc 3, 67400, Illkirch-Graffenstaden, France

Correspondence
Marine Froissard and Jean-Denis Faure, Université Paris-Saclay, INRAE, AgroParisTech, Institut Jean-Pierre Bourgin (IJPB), Versailles, France.
Email: marine.froissard@inrae.fr and jean-denis.faure@agroparistech.fr

Chouaib Meziadi, Core Biogenesis, Illkirch Graffenstaden, France.
Email: chouaib.meziadi@corebiogenesis.com

Present address
Lionel Gissot, The University of Iowa, Iowa City, USA
Ousmane Dao, Aix Marseille Univ, CEA, CNRS, Institut de Biosciences et Biotechnologies Aix-Marseille, CEA Cadarache, Saint-Paul-lez-Durance, France

Lionel Gissot and Florent Fontaine co-first authors.

Funding information
Merck KGaA, frankfurter straße 250 64293 darmstadt; Saclay Plant Sciences (SPS), Grant/Award Number: ANR17-EUR-007

Abstract

Plants are gaining traction as a cost-effective and scalable platform for producing recombinant proteins. However, expressing integral membrane proteins in plants is challenging due to their hydrophobic nature. In our study, we used transient and stable expression systems in *Nicotiana benthamiana* and *Camelina sativa* respectively to express SARS-CoV-2 E and M integral proteins, and target them to lipid droplets (LDs). LDs offer an ideal environment for folding hydrophobic proteins and aid in their purification through flotation. We tested various protein fusions with different linkers and tags and used three dimensional structure predictions to assess their effects. E and M mostly localized in the ER in *N. benthamiana* leaves but E could be targeted to LDs in oil accumulating tobacco when fused with oleosin, a LD integral protein. In *Camelina sativa* seeds, E and M were however found associated with purified LDs. By enhancing the accumulation of E and M within LDs through oleosin, we enriched these proteins in the purified floating fraction. This strategy provides an alternative approach for efficiently producing and purifying hydrophobic pharmaceuticals and vaccines using plant systems.

KEYWORDS
camelina, colabfold, Goldenbraid, lipid droplet, SARS-CoV-2, tobacco

1 | INTRODUCTION

Plants have been used successfully over years as a platform for expressing recombinant proteins.[1] Plants provide cost-effectiveness, scalability and safety of production since they can be grown on a large

Abbreviations: ACE-2, angiotensin-converting enzyme-2; E, envelope; ER, endoplasmic reticulum; GFP, green fluorescent protein; LD, lipid droplet; LDAP, lipid droplet associated protein; M, membrane; MDH, monodansylpentane;; mRFP1, monomeric red fluorescent protein 1; N, nucleocapsid; S, spike; TAG, triacylglycerol; VLP, virus like particles.

scale, and are devoided of human and animal pathogens. Several systems were developed including transient expression in tobacco leaves for their fast production schemes or stable transformants for the possibility of extensive culture.[2] Plants were used for the production of a large set of proteins for functional analysis including enzymes, transcription factors, structural proteins but also recombinant proteins for commercial production that mostly targeted high-value biopharmaceutical products.[1] Recombinant protein production in plants faces two challenges: protein yield and purification, mostly caused by the large size of plant cells and the elimination of large quantities of insoluble debris.

To bypass some of these limitations, lipid droplets (LDs) accumulated in oilseed plants have been used as a scaffold system to accumulate recombinant proteins.[3] LDs have been used in biotechnology for reconstructing and channeling metabolic pathways.[4–6] LDs have also been used to express, anchor and purify protein of interest like growth factors in arabidopsis, camelina and safflower.[7–10] LDs can be accumulated not only in seeds but also in leaves, providing an alternative and even faster way for testing protein targeting.[11] The main structural LD proteins in plants are the oleosins and their related proteins (caleosin and stereoleosin), the LD Associated proteins (LDAP), as well as enzymes like dioxygenase.[12] LDs could therefore be used for targeting Integral membrane proteins with other structural features either directly or by the means of LD structural proteins. The rationale is that targeting LDs could promote both the integral membrane protein accumulation by providing the ad hoc hydrophobic environment, as well as their purification scheme by taking advantage of flotation fractionation. This hypothesis was therefore tested with the two integral membrane proteins E and M from the SARS-CoV-2 since plants could be a valuable source of viral proteins as vaccine immunogens.[13–18]

The SARS-CoV-2 membrane (M) protein contributes in the formation of the viral membrane that formed the mature virus particles.[19] The envelope (E) protein is involved in the formation of the virus particles.[20] The M protein is the most abundant viral protein of SARS-CoV-2, and is involved in multiple viral functions like the initial attachment to the host cell and the viral protein assembly.[21] The E protein is the smallest of the four structural viral proteins with 76 amino acids and is involved in assembly, budding, envelope formation, and pathogenesis of the virus.[22] E and M proteins are integral membrane proteins that are difficult to express and purify, but several models have predicted 1 and 3 transmembrane domains respectively.[21,23–25] Plants have already been used as vectors to develop vaccines in particular against SARS-CoV-2 virus.[26–28] Different strategies were developed including isolated recombinant S proteins,[29,30] virus-like particles (VLP)[31–33] receptor binding domain and neutralizing monoclonal antibody.[34] However, most of the vaccine strategies relied on S protein recognition by the immune system which is prone to genetic variation.[35] Having access to purified core SARS-CoV-2 E and M structural proteins that are more genetically stable compared to S would be valuable to develop alternative therapeutic and vaccine strategies. Contrary to S proteins, M and E proteins are strongly conserved and showed low occurrence of variants[22,36,37] and at least for M protein is still immunogenic albeit at a much lower rate compared to S.[38,39]

We evaluated different strategies to express and enrich E and M proteins in plant extracts and we developed an extensive analysis of the optimal constructs combining different tags and linkers to be expressed transiently in tobacco leaf as well as in stable camelina transgenic seeds. Both E and M proteins associated with plant LDs after flotation enrichment, but their fusions with oleosins enhanced their targeting to LDs. These results demonstrate the interest of LDs for recombinant integral membrane protein expression.

2 | RESULTS

2.1 | A synthetic biology pipeline for expressing fusion proteins in plants

Modified Goldenbraid technology was used for combinatorial association of different coding parts (target proteins, labeling tags, targeting anchors, linkers) with promoters and terminators in plants.[40,41] To further extend the combinatory assembly of coding parts, two new suffix/prefix were introduced (GCAG, Gln and GGTA, Val) in complement of the four existing extensions (AATG,Met; AGCC, Ala; TTCG, Ser; GCTT, Stop) allowed the assembly of up to five different parts within the coding sequence (Figure 1). A full transcriptional unit could be assembled with a total of eight suffix/prefix positions labelled S1 to S8 that includes promoter and terminator positions. These different constructs were expressed under the control of the *Arabidopsis thaliana* pAtUBI10 promoter/35S terminator and the *Glycine max* pGlycinin promoter/terminator for the expression in *N. benthamiana* leaves and *C. sativa* seeds respectively.[42,43] A total of 30 constructs were assembled for the expression in *N. benthamiana* using the 2 SARS-CoV-2 E and M proteins in combinations with tags, linkers and lipid droplet anchor (AtOLE1) (Figure 2A; Table ST1 A and B). Another subset of seven constructs for *C. sativa* seed expression was also made (Figure 2A; Table ST1). Finally, a specific construct based on PUSH/PULL/PROTECT strategy with three transcriptional units expressing MmFIT2, MmDGAT2, AtWRI1 was assembled to induce LD formation in *N. benthamiana* leaves.[44,45]

The different combinations of SARS-CoV-2 proteins with tags and linkers were tested in transient expression in *N. benthamiana* leaves (Figure 1B). Subcellular distribution of constructs with fluorescent tags were checked by confocal microscopy and the expression level was monitored by western blot. For HA constructs, only western blot analysis was carried out.

Only constructs with HA or AtOLE1 LD anchor were subsequently tested in camelina seeds (Figure 1C). For each construct, a total of 24 T1 plants were produced and their progeny (T2 seeds) were screened for the presence of recombinant protein in total seed extract. At least the two best lines were kept for LD purification and analysis.

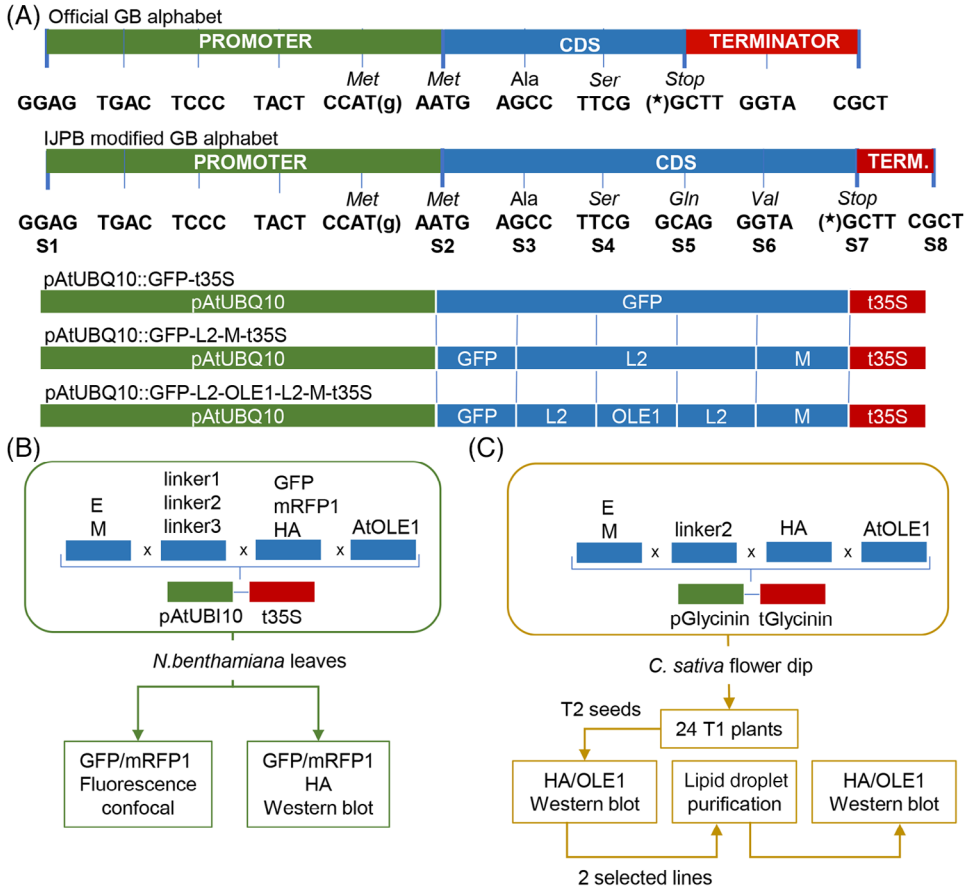

FIGURE 1 Recombinant expression cloning and expression. (A) Modified Goldenbraid (GB) alphabet used to assemble protein modules. Construct assembly and phenotyping for their transient expression in *N. benthamiana* (B) leaves and stable expression in *C. sativa* seeds (C). The different GB parts (blue box) could be combined (x) with promoters (green box) and terminators (red box).

2.2 | Expression of E and M fusion proteins in transient tobacco leaf system

Transient assay in *N. benthamiana* was used to assess the most efficient combinations of SARS-CoV-2 proteins with fluorescent tags and linkers for protein expression in plant cells. The E and M proteins fused with either GFP or mRFP1 showed different subcellular distribution according to the position of the fluorescent protein (N- or C-terminus) and the nature of the linker (Figure 2A and Figure S1A, B). Overall, the two proteins were mostly accumulated in the ER, nucleus and in unidentified vesicles that were different from plastids, golgi, and peroxisomes (Figure 2B and 2C).

We then compared subcellular distribution of the fusion proteins with their accumulation in total leaf extracts (Figure 2A, D and E; Figure S1A-D). When E and M proteins were positioned at the N-terminus of the fusion proteins, they showed a globally higher occurrence of protein accumulation (X-L-Tag, 10 out of 12 combinations) compared to C-terminus fusion (Tag-L-X, 6 out of 12 combinations). Moreover, positioning E and M proteins at the C-terminus of the fusion protein increased the occurrence of double bands in western blots (4/12) compared to N-terminus (0/12) indicating possible proteolytic cleavage (Figure 2A; Figure S2C-D). The short and flexible linker 2 improved protein expression in both N- and C-terminal fusions compared to linker 1 (long and flexible) and linker 3 (short and bent). In conclusion, E protein was mostly accumulated in ER, nucleus and unidentified vesicles while M protein was mostly found in ER and unidentified vesicles (Figure 2A and 2B).

To better assess the impact of the different linkers, we predicted the three-dimensional (3D) structure of the different fusion proteins using the Colabfold portal combining the highly efficient RoseTTAfold and AlphaFold2 predicting algorithms.[46] The structure of E and M SARS-CoV-2 proteins fused to different linkers and fluorescent proteins (GFP and mRFP1) was predicted with a high level of confidence as indicated by the high pLDDT index value (Figure S2 and S3). E protein was predicted as a single alpha helix while M protein showed three alpha helices in "Z" shape followed by a beta sheets domain (Figure 3). Even if linker structures were more difficult to predict, fusion protein structure seemed to be significantly impacted by the linker nature (Figure 3; Figure S2 and S3). Such structural changes could explain the observed difference in localization and protein accumulation of E and M fusion proteins. For instance, for GFP-linker-E protein configuration, only the short, flexible linker 2 enabled significant accumulation of E

(A)

		Constructs	Fluorescence localization						Western blot
			ER	n.d. vesicles	cytosol	nucleus	LDs	Large vesicles	Total extract
N. benthamiana leaves		GFP-L1-E	✓		✓	✓			
		GFP-L2-E	✓						++*
		GFP-L3-E			✓	✓			
		E-L1-GFP			✓	✓			
		E-L2-GFP		✓		✓			+
		E-L3-GFP			✓	✓			
		GFP-L1-M	✓		✓	✓			
		GFP-L2-M	✓						++
		GFP-L3-M			✓	✓			
		M-L1-GFP	✓	✓					++
		M-L2-GFP	✓	✓					++
		M-L3-GFP			✓	✓			++
		mRFP1-L1-E	✓						++*
		mRFP1-L2-E	✓	✓					++*
		mRFP1-L3-E	weak						+*
		E-L1-mRFP1			✓	✓			+
		E-L2-mRFP1	✓	✓					+
		E-L3-mRFP1			✓	✓			++
		mRFP1-L1-M	✓			✓			
		mRFP1-L2-M	✓						+
		mRFP1-L3-M	weak						
		M-L1-mRFP1	✓						++
		M-L2-mRFP1	✓						++
		M-L3-mRFP1	✓						++
		HA-E							
		E-HA							+
		HA-M							
		M-HA							++
	+ LDs	E-L2-GFP	✓	✓				✓	
		M-L2-GFP	✓	✓					
		E-L2-mRFP1	✓	✓				✓	
		M-L2-mRFP1	✓	✓					
		E-L2-OLE1-L2-GFP		✓			✓		
		M-L2-OLE1-L2-GFP		✓					
									LD extract
C. sativa seeds		E-HA							+/-
		M-HA							+
		E-L2-OLE1							
		OLE1-L2-E							++
		M-L2-OLE1							++
		OLE1-L2-M							

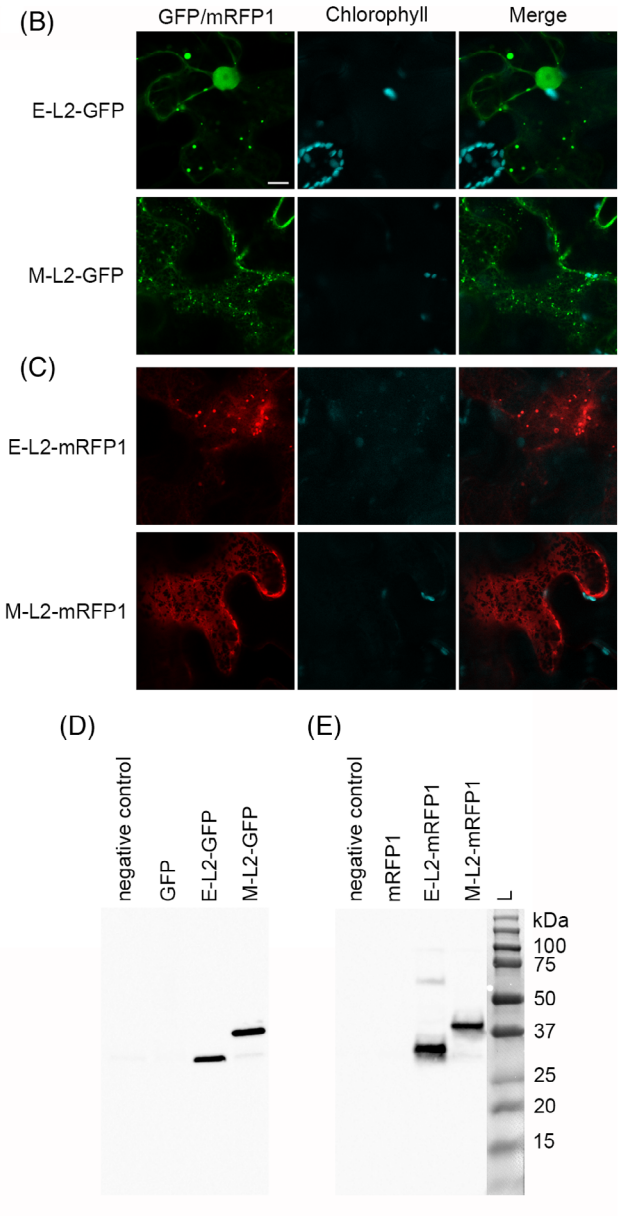

FIGURE 2 Localization and accumulation of E and M fusion proteins in *N. benthamiana* leaves. (A) Summary of confocal subcellular localization and/or western blot expression of all E and M fusion proteins in wild-type and oil accumulating *N. benthamiana* leaves, and *C. sativa* seeds.. Qualitative expression level was expressed as +/-, +, and ++, as determined using western blot experiments. Stars (*) indicate the presence of double bands on western blots. ER, endoplasmic reticulum; n.d. vesicles, not determined vesicles; LD, lipid droplets. (B-C) Subcellular distribution of GFP- (B) or mRFP1- (C) fusion proteins with E and M. (D-E) Accumulation of GFP- (D) and mRFP1- (E) fusion with E and M. Western blot analysis using an anti-GFP (D) and -mRFP1 (E) monoclonal antibody. Scale bar, 10 µm.

protein and its localization in the ER and unidentified vesicles. Linker 2 led to a fusion protein in which GFP was further away from E protein alpha helix structure compared to the two other linkers (Figure 3). The mRFP1-L2-E protein localized in the ER but with significant proteolytic cleavage suggesting a non-optimal configuration of the protein. Interestingly, mRFP1 protein was predicted to be closer to the E protein alpha helix withlinker 2. The linker effect was also important for GFP-Linker-M fusion proteins even if the structural reasons for the defective localization and low protein accumulation were not as clear as for the E protein.

2.3 | Targeting E and M to LDs in transient oil accumulating tobacco leaves

Considering the hydrophobic properties of E and M integral membrane domains, we tested whether these SARS-CoV-2 proteins could be targeted to LDs. All E/M constructs were co-expressed with FIT2/DGAT2/WRI1, that induce LD accumulation in tobacco leaves like in oleaginous seeds. As previously described, E and M fused with GFP tag were found in the ER and in unidentified vesicles (Figure 4A). However, E-L2-GFP protein (Figure 4A, upper panels) and M-L2-GFP

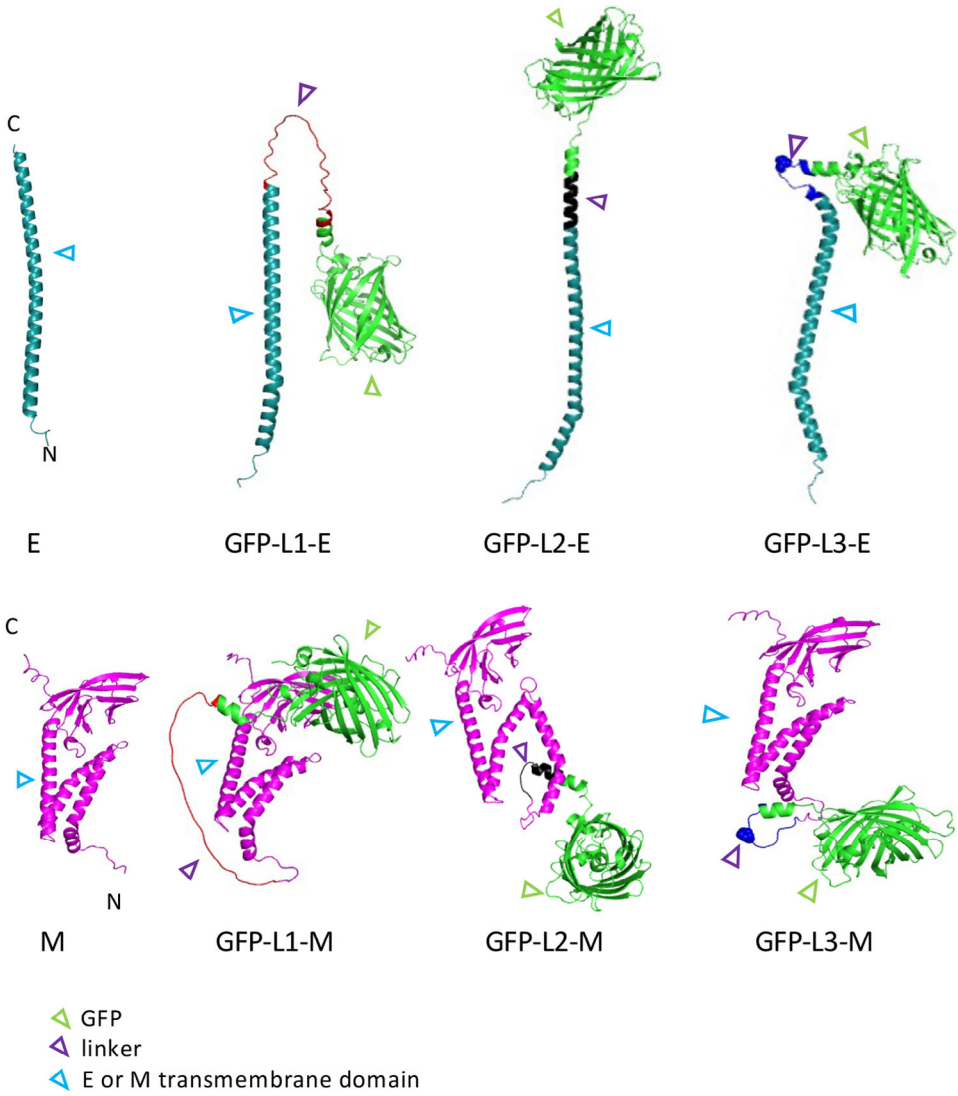

FIGURE 3 Predicted three-dimensional structure of GFP-linker-E and -M proteins. Protein structures were predicted by Colabfold and the different protein modules were identified by specific colors using PyMol. E (blue), M (pink), GFP (green), linker 1 (orange), linker 2 (black), and linker 3 (dark blue).

protein (Figure 4A, lower panels) could not be co-localized with LDs, as assessed with the neutral lipid marker MDH (Monodansylpentane). E-L2-GFP and E-L2-mRFP1 proteins were nonetheless observed at the surface of large vesicles (± 1 µm) structurally different from the unidentified vesicles observed previously but also from LDs labelled with MDH (Figure S4).

To efficiently target E and M proteins to LD, E and M proteins were fused with Linker 2 to the main Arabidopsis seed oleosin AtOLE1. We used the E/M-L2-AtOLE1-L2-GFP fusion protein configuration since AtOLE1 is known to have a central hairpin structure with free cytosolic N- and C-terminus. E/M proteins were preferentially associated at the N-terminus of the fusion protein as previously shown. No colocalization with MDH was observed for M-L2-OLE1-L2-GFP protein (Figure 4B, lower panels) and a partial colocalization with MDH was observed for E-L2-OLE1-L2-GFP protein (Figure 4B, upper panels) as confirmed by Pearson's correlation coefficients (Figure S5).

2.4 | Expression of E and M fusion proteins in *C. sativa* seeds

We then checked whether E and M proteins could be expressed in seeds. To minimize the tag interference observed with GFP and mRFP1 (Figure 2A), E and M proteins were directly fused with an HA tag at both N- and C-terminus. The four different fusions were first tested in LD-accumulating *N. benthamiana*. As expected, the most efficient accumulation of E and M proteins was associated with the C-terminal position of the tag even as small as HA (Figure 5A). M-HA protein was found to be more strongly accumulated in leaves than E-HA protein while HA-E protein and HA-M protein could not even be detected. E-HA and M-HA proteins were then expressed camelina under the control of seed storage protein promoter/terminator and successfully detected in crude seed extracts (Figure 5B, left). LD purified by flotation from few seeds with an adapted protocol led to the expected

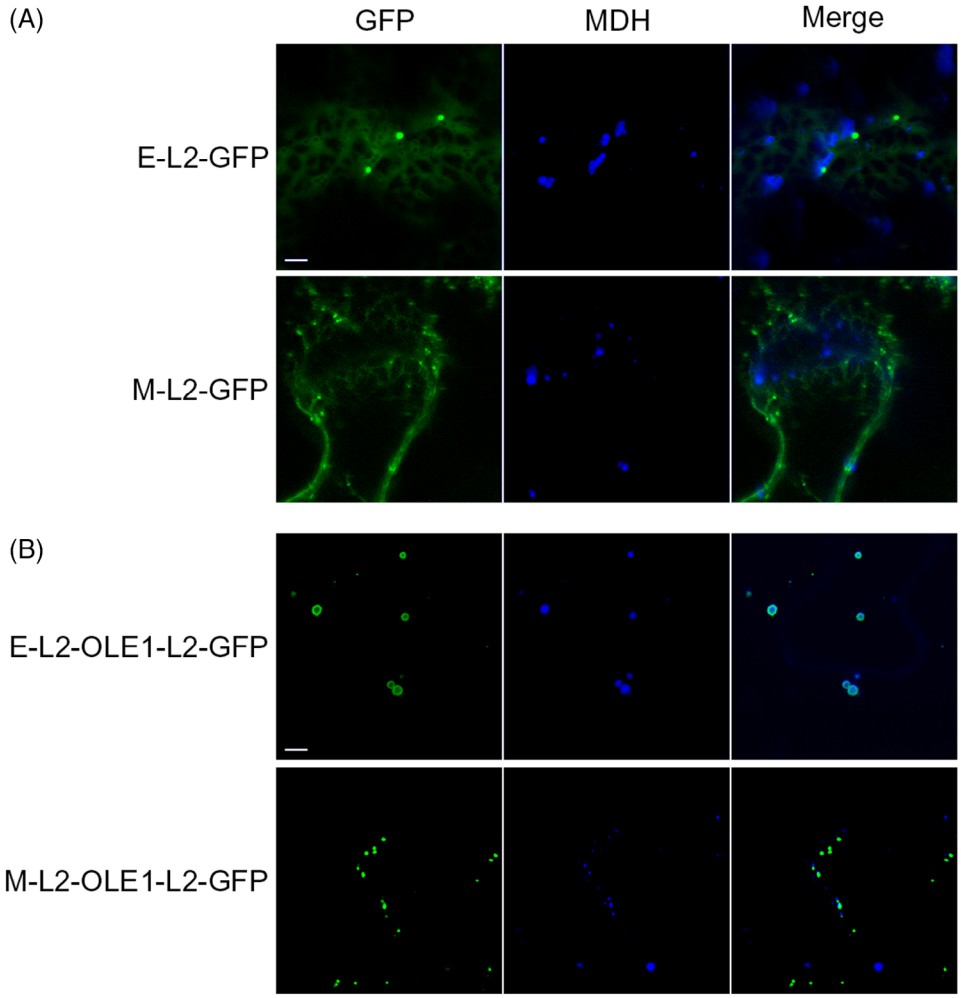

FIGURE 4 Confocal subcellular colocalization of E and M fusion proteins in *N. benthamiana* leaves with lipid droplets. E-L2-GFP (A, upper panels), M-L2-GFP (A, lower panels), E-L2-OLE1-L2-GFP (B, upper panels) and M-L2-OLE1-L2-GFP (B, lower panels), were colocalized with monodansylpentane (MDH). Scale bar, 5 μm.

protein profile compared to crude seed extract (Figure S6A). Like for *N. benthamiana*, M-HA protein seems to be more efficiently accumulated than E-HA protein but both M-HA and E-HA proteins could be recovered in LD fractions (Figure 5B, right). Protein fusions with AtOLE1 at N- or C-terminal position were also expressed in camelina but only OLE1-L2-E and M-L2-OLE1 fusion proteins could be detected (alone or combined) in crude T2 seed extracts (Figure 5C, right; Figure S6B). Interestingly, unlike the HA fusion proteins, the AtOLE1 anchoring favored the accumulation of E and M proteins at the same level in the LD fraction (Figure 2A and 5C, right). The predicted structure of the fusion proteins showed that AtOLE1 "V" shaped alpha-helices inserted in the LD membrane were always in the same plane as the E and M alpha helices (Figure S7). Such a co-alignment configuration of alpha-helices could favor insertions of both AtOLE1 and M membrane domains into the LD phospholipid monolayer (Figure S7). It has to be noted that M-L2-OLE1 protein showed a lower size as expected. The fusion protein with a theoretical molecular weight of 44 kDa showed an apparent size of about 33 kDa. However, both N- and C-terminal of M moiety were present when analyzed by mass-spectrometry indicating that the complete M protein sequence was present within the fusion protein (Figure S8).

The best camelina lines expressing the highest level of E and M proteins in seeds were grown to obtain homozygous T3 seed progeny. After line screening for recombinant proteins expression using western-blot (Figure S9A, B), seed LDs were purified. Coomassie blue protein profiles were analyzed to detect any additional band corresponding to recombinant proteins. E-HA, M-HA, OLE1-L2-E proteins were not detected on protein profiles due to their low accumulation or possible co-migration with major LD proteins (Figure 5D; Figure S9C). A band corresponding to M-L2-OLE1 protein was nonetheless detected at 33 kDa (Figure 5D, E) and its accumulation was evaluated at 1% of total LD proteins (Figure 5D, E; Figure S9D, E). Sonication of wet seeds to remove mucilage prior to LD extraction was performed and slightly improved M-L2-OLE1 protein recovery, with 1.5 ± 0.1% ($n = 4$) compared to 1.0 ± 0.1% ($n = 4$) without sonication (Figure 5E).

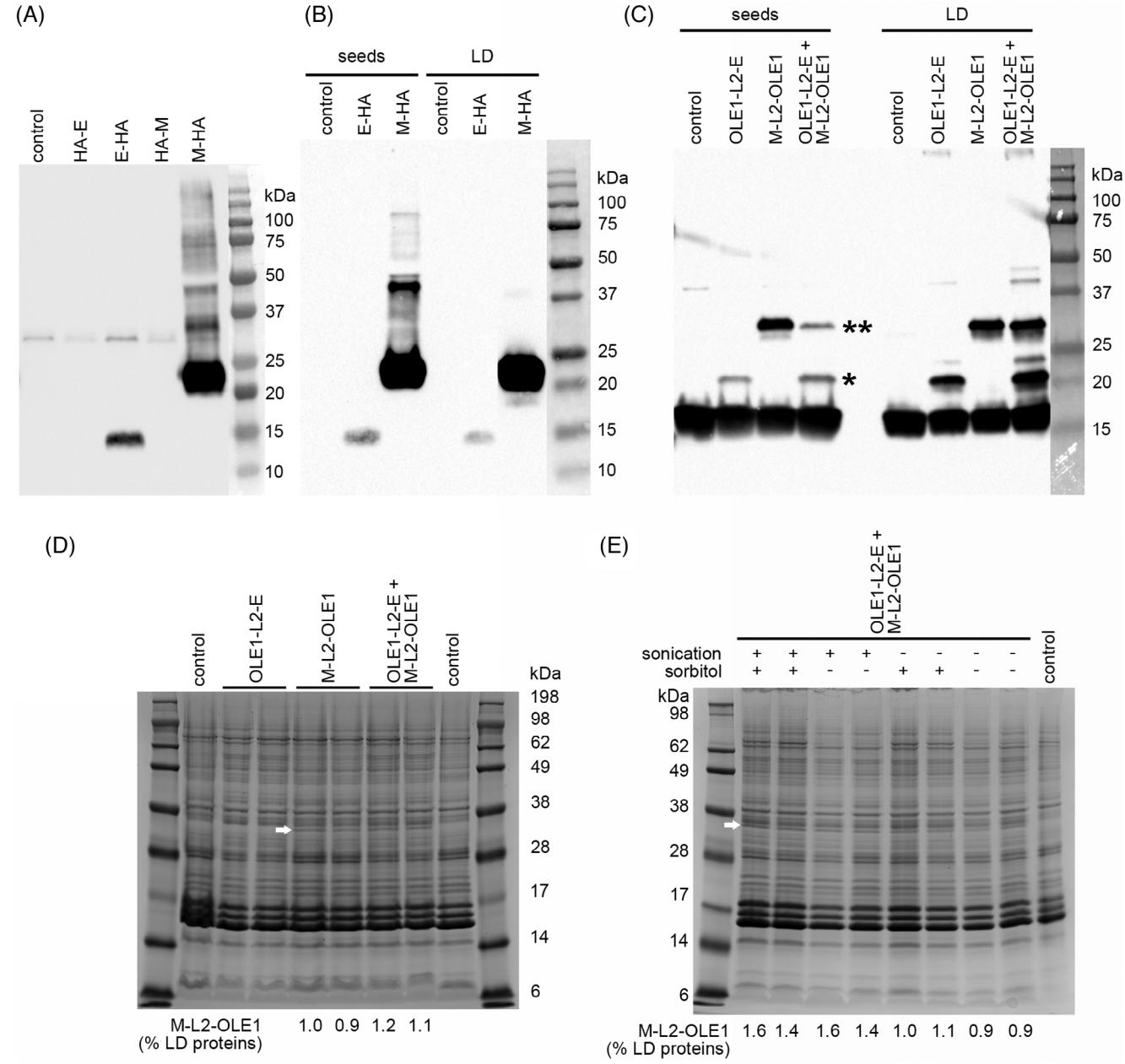

FIGURE 5 Expression of E and M protein fusion in *N. benthamiana* leaves, camelina T2 and T3 seeds. (A) HA tagged E and M fusion proteins in *N. benthamiana* leaves. (B) HA tagged E and M fusion proteins in camelina seeds and purified LDs. Fusion proteins were visualized using immunoblot with monoclonal anti-HA antibodies (C) Accumulation of E (*) and M (**) protein fusion with AtOLE1 in camelina seeds and purified LDs. Fusion proteins were detected using immunoblot with anti-AtOLE1 polyclonal antibody. LD proteins form T3 seeds expressing OLE1-L2-E and M-L2-OLE1 fusion proteins were visualized on Coomassie staining polyacrylamide gels using conventional extraction protocol (D) and with a modified protocol, with or without sonication for mucilage removing and with or without sorbitol in the buffer (E). The M-L2-OLE1 band signal (arrow) was quantified as a percentage of total LD protein signal on Coomassie staining polyacrylamide gels. The result was presented under each profile analyzed.

3 | DISCUSSION

The expression of SARS-CoV-2 E and M proteins were successfully achieved in two different plant systems. *N. benthamiana* leaves have efficiently expressed several viral proteins including SARS-CoV-2 proteins but only M and N proteins could be detected in the plant extracts.[16,29,32,34,47] We found that E fusion proteins were difficult to accumulate in both plant systems except when associated with LD anchor protein like AtOLE1. AtOLE1 could not only help targeting E protein to LDs but also could stabilize the fusion protein in seed LDs. Indeed, seeds could be seen as a better system for recombinant protein expression since they naturally accumulate very high levels of storage proteins and have low protease activity and water content.[48] Moreover seeds are also able to store recombinant proteins for years at

ambient temperature (for review see[49]). Since M could be quantified in seed LD extract, its theorical production yield could therefore be calculated. The approximate LD protein content in seeds were estimated at 5.5 and 36 mg g^{-1} of seeds for respectively arabidopsis and rapeseed.[50,51] Therefore, the theorical yield for the expression and purification of M protein could be estimated between 82.5 and 540 mg kg^{-1} seeds. High yield is defined for the expression and purification of recombinant proteins above 100 mg kg^{-1} of plant material as achieved for instance for soluble antibodies.[1] Since camelina was described to achieve seed yield in fertilized conditions around 1300 and 3300 kg ha^{-1}, the theorical production for M protein at a farm scale would be between 100–270 to 700–1800 g ha^{-1}.

Even in the most favorable plant systems, the structure of recombinant protein fusion has a strong impact on protein accumulation. We showed here that the nature of tags and linkers and their relative positions in the fusion construct could modify not only the protein subcellular distribution but also its stability. Some of the most favorable fusion protein structures require to have tags at the C-terminus of the fusion protein. We previously showed that tag position needed to be tested in all configurations since efficient targeting will be dependent on the domain/protein used as well as its position in the construct.[52] We also found that the use of a short flexible linker improved E and M protein accumulation. Longer flexible linkers could offer a larger mobility and array of freedom between protein modules. It could also interfere with folding processes like for membrane integration. A short but bent linker like linker 3 creates topology limitations that could also interfere with protein membrane interactions. Linkers are often neglected even if they are known to impact recombinant protein expression and extensive combinatorial assembly is essential to optimize each linker with the corresponding fused parts.[53]

In most construct configurations, E and M proteins were found to localize in the ER which is not surprising since it is the site of SARS-CoV-2 protein synthesis and assembly of the virus particle before entering the secretory pathway in mammalian cells.[54] The association of E and M with LD fractions in camelina seeds could be explained by the ER origin of these structures. The massive LD budding process in the course of seed development could drag ER integral proteins and trap them into LDs. LD relocation of membrane proteins from the secretory pathway upon physiological modifications was also previously documented for caveolin in mammals[55] or SNA2 in yeast.[56] Alternatively, it is known that some viruses like hepatitis C could hijack cell LDs for the assembly of infectious particles via direct interaction of viral proteins with LDs.[57] The SARS-CoV-2 viruses were also found to colocalize with LDs in infected vero cells and the reduction of LD formation inhibited virus replication.[58] Furthermore, M protein was found to colocalize with accumulated LD-like structures containing neutral lipids in infected vero cells indicating that M has a natural protein affinity for LD hydrophobic environment.[59]

In conclusion, the association of the anchor protein AtOLE1 improves E and M protein targeting, demonstrating that plant oleosin could be used to efficiently scaffold viral integral membrane protein on LDs. LDs simplify protein purification thanks to the flotation partitioning method and opens the way to alternative platforms using oilseed for recombinant hydrophobic protein production.

4 | MATERIALS AND METHODS

4.1 | Plant materials and growth conditions

Camelina sativa cv Celine plants were grown and transformed as described in.[60] *Nicotiana benthamiana* plants were grown and agroinfiltrated as described in.[61]

4.2 | GoldenBraid cloning

All the GB reactions (domestication of the part, creation of the transcribed unit (TU) and multigene assembly) were performed in a Thermofisher thermocycler according to the protocols described in the Goldenbraid 4.0 internet site (https://gbcloning.upv.es/). Primers used are listed in Table ST2. The promoter/terminator parts are available from addgene (https://www.addgene.org/). Plasmids used to create the TU or the multigene assembly were pDGB3 series. The Sars-Cov-2 sequences were OP218757 for M and OP161148 for E. E and M protein sequences were synthetized (TwistBioscience, San Franscisco, California) with plant codon optimization.

4.3 | Confocal imaging of GFP/mRFP1 constructs

oil accumulating *N. benthamiana* were infiltrated with a solution of 0.3 µM of monodansylpentane (MDH, Autodot, Abcepta) 5 min before observation. Observations were carried out with Leica SP5 or SP8 AOBS confocal laser microscopes using either a PL APO 63 × 1.20 NA or 20 × 0.75 NA water-immersion objectives. The respective excitation/emission parameters (nm) are: GFP (488, 495–550), mRFP1 (561, 600–625), autofluorescence (488, 700–750), and MDH (405 nm, 420–480). Colocalization between XFP/MDH was evaluated using the Pearson's coefficient correlation delivered by the Fiji JaCoP plugin ,[62] Kruskal-Wallis' test (p value $< 2.2^{e-16}$) and a pairewise Wilcoxon's test.

4.4 | Protein folding prediction

Protein folding prediction was performed using ColabFold:AlphaFold2 (number of cycles, 6; dpi, 500). The query sequences are provided in File SF1. The confidence measure was provided by the predicted local distance difference test (pLDDT) and used to colour-code the residues of the model in the three dimensional structure viewer.

4.5 | Total seed protein extracts

Total seed protein extracts (two seeds) were prepared as described previously.[63]

4.6 | LD purification

After water imbibition 30 min at 4°C and a 30 s optional sonication for mucilage removing, a total of five seeds for screening (~5.75 mg) or 10 seeds for LD protein profile analysis (~11.5 mg) were processed as described in.[63]

4.7 | SDS PAGE and Immunoblotting

Proteins were separated by SDS-PAGE using ready-to-use mini PROTEAN TGX Stain Free gels (BioRad) for screening and NuPAGE Bis-Tris gels (ThermoFisher) for LD protein profile analysis according to the manufacturer's instructions. For immunoblotting experiments, proteins were probed with monoclonal antibodies raised against HA (clone 3F10, rat IgG, Roche), GFP (clone 3H9, rat IgG, Chromotek) and polyclonal antibodies raised against DsRed/mRFP1 (Rabbit serum, Rabbit ID 1510004, Takara) and AtAtOLE1.[64] Primary antibodies were detected using horseradish peroxidase-conjugated anti-rat (goat IgG, 31470, Thermo Scientific) and anti-rabbit IgG (Goat IgG, SAB3700878, Sigma-Aldrich) secondary antibodies and revealed using Clarity Western ECL Substrate (BioRad). Stain Free staining and luminescence from peroxidase activity were recorded using the ChemiDoc MP Imaging System (BioRad). LD protein profile analysis was performed on Coomassie blue stained gels using Image Lab Software (BioRad).

4.8 | Mass spectrometry

Coomassie blue stained protein bands on SDS PAGE were excised, washed with ethanol and dry. At the proteomics platform, in-gel digestion was then performed with trypsin (cleavage site = K/R) or lysC (cleavage site = K). For the mass spectrometry (MS) analysis, the recovery volume was 20 µL 0.1% TFA and the injection volume was 1 µL. The instrument Orbitrap ELITE/C18 Accucore 50-cm column was used. 2 h run mass spectrum analyzer and Top20CID method were used. For the data processing, software Proteome Discoverer 2.4 (Sequest HT/Percolator) was used, with the thresholds of 1% false discovery rate, minimum of 1 peptide per protein. Databases used were contaminants_190528.fasta; Camelina_sativa_211213_ensembl.fasta, SARS-CoV-2_Uniprot_reviewed_220207.fasta.

AUTHOR CONTRIBUTIONS

Lionel Gissot: Conceptualization; Investigation; Methodology; Resources; Writing – original draft. Florent Fontaine: Formal analysis; Investigation; Methodology; Visualization; Writing – original draft. Zsolt Kelemen: Conceptualization; Investigation; Methodology; Resources. Ousmane Dao: Investigation; Resources. Isabelle Bouchez: Methodology; Resources. Carine Deruyffelaere: Investigation; Resources. Michèle Winkler: Investigation; Resources. Fabienne Pierre: Investigation; Resources. Chouaib Meziadi: Conceptualization; Project administration; Supervision; Validation; Writing – review & editing. Jean-Denis Faure: Conceptualization; Project administration; Supervision; Validation; Writing – original draft; Writing – review & editing. Marine Froissard: Conceptualization; Funding acquisition; Investigation; Methodology; Project administration; Resources; Supervision; Validation; Writing – original draft; Writing – review & editing

ACKNOWLEDGMENTS

The authors thank Patrick Grillot, Hervé Ferry and IJPB Observatoire du végétal staff for smooth running of the facilities, Jasmine Burguet for helpful discussions on image analysis, Merck for their financial support. The IJPB benefits from the support of the Labex Saclay Plant Sciences-SPS (ANR-17-EUR-0007). The authors acknowledge Biorender for Graphical abstract design.

CONFLICT OF INTEREST STATEMENT

The authors declare that they have no conflict of interest.

DATA AVAILABILITY STATEMENT

Data available in article supplementary material.

ORCID

Marine Froissard https://orcid.org/0000-0002-6194-9477

REFERENCES

1. Schillberg, S., Raven, N., Spiegel, H., Rasche, S., & Buntru, M. (2019). Critical analysis of the commercial potential of plants for the production of recombinant proteins. *Frontiers in Plant Science*, *10*, 720. https://doi.org/10.3389/fpls.2019.00720
2. Burnett, M. J. B., & Burnett, A. C. (2020). Therapeutic recombinant protein production in plants: Challenges and opportunities. *Plants, People, Planet*, *2*(2), 121–132. https://doi.org/10.1002/ppp3.10073
3. Bhatla, S. C., Kaushik, V., & Yadav, M. K. (2010). Use of oil bodies and oleosins in recombinant protein production and other biotechnological applications. *Biotechnology Advances*, *28*(3), 293–300. https://doi.org/10.1016/j.biotechadv.2010.01.001
4. Lin, J. L., Zhu, J., & Wheeldon, I. (2017). Synthetic protein scaffolds for biosynthetic pathway colocalization on lipid droplet membranes. *ACS Synthetic Biology*, *6*(8), 1534–1544. https://doi.org/10.1021/acssynbio.7b00041
5. Sadre, R., Kuo, P., Chen, J., Yang, Y., Banerjee, A., Benning, C., & Hamberger, B. (2019). Cytosolic lipid droplets as engineered organelles for production and accumulation of terpenoid biomaterials in leaves. *Nature Communications*, *10*(1), 853. https://doi.org/10.1038/s41467-019-08515-4
6. Shi, Y., Wang, D., Li, R., Huang, L., Dai, Z., & Zhang, X. (2021). Engineering yeast subcellular compartments for increased production of the lipophilic natural products ginsenosides. *Metabolic Engineering*, *67*, 104–111. https://doi.org/10.1016/j.ymben.2021.06.002
7. Cai, J., Wen, R., Li, W., Wang, X., Tian, H., Yi, S., Zhang, L., Li, X., Jiang, C., & Li, H. (2018). Oil body bound oleosin-rhFGF9 fusion protein expressed in safflower (Carthamus tinctorius L.) stimulates hair growth and wound healing in mice. *BMC Biotechnology [Electronic Resource]*, *18*(1), 51. https://doi.org/10.1186/s12896-018-0433-2
8. Gao, H., Wang, F., Hu, X., Li, Y., Zhang, Y., Carther, K. F. I., Wang, B., Min, F., Wang, X., Wu, H., Xu, K., Zhou, Y., Liu, X., Li, X., & Li, H. (2021). Camelina lipid droplets as skin delivery system promotes wound repair by enhancing the absorption of hFGF2. *International Journal of*

Pharmaceutics, *598*, 120327. https://doi.org/10.1016/j.ijpharm.2021.120327

9. Qiang, W., Gao, T., Lan, X., Guo, J., Noman, M., Li, Y., Guo, Y., Kong, J., Li, H., Du, L., & Yang, J. (2020). Molecular pharming of the recombinant protein hEGF-hEGF concatenated with oleosin using transgenic arabidopsis. *Genes*, *11*(9), 959. https://doi.org/10.3390/genes11090959
10. Yang, J., Qiang, W., Ren, S., Yi, S., Li, J., Guan, L., Du, L., Guo, Y., Hu, H., Li, H., & Li, X. (2018). High-efficiency production of bioactive oleosin-basic fibroblast growth factor in A. thaliana and evaluation of wound healing. *Gene*, *639*, 69–76. https://doi.org/10.1016/j.gene.2017.09.064
11. Pyc, M., Cai, Y., Greer, M. S., Yurchenko, O., Chapman, K. D., Dyer, J. M., & Mullen, R. T. (2017). Turning over a new leaf in lipid droplet biology. *Trends in Plant Science*, *22*(7), 596–609. https://doi.org/10.1016/j.tplants.2017.03.012
12. Huang, A. H. C. (2018). Plant lipid droplets and their associated proteins: Potential for rapid advances. *Plant Physiology*, *176*(3), 1894–1918. https://doi.org/10.1104/pp.17.01677
13. Ataie Kachoie, E., Behjatnia, S. A. A., & Kharazmi, S. (2018). Expression of human immunodeficiency virus type 1 (HIV-1) coat protein genes in plants using cotton leaf curl Multan betasatellite-based vector. *PLoS ONE*, *13*(1), e0190403. https://doi.org/10.1371/journal.pone.0190403
14. Margolin, E., Chapman, R., Williamson, A.-L., Rybicki, E. P., & Meyers, A. E. (2018). Production of complex viral glycoproteins in plants as vaccine immunogens. *Plant Biotechnology Journal*, *16*(9), 1531–1545. https://doi.org/10.1111/pbi.12963
15. Matić, S., Masenga, V., Poli, A., Rinaldi, R., Milne, R. G., Vecchiati, M., & Noris, E. (2012). Comparative analysis of recombinant Human Papillomavirus 8 L1 production in plants by a variety of expression systems and purification methods. *Plant Biotechnology Journal*, *10*(4), 410–421. https://doi.org/10.1111/j.1467-7652.2011.00671.x
16. Park, Y., An, D.-J., Choe, S., Lee, Y., Park, M., Park, S., Gu, S., Min, K., Kim, N. H., Lee, S., Kim, J. K., Kim, H.-Y., Sohn, E.-J., & Hwang, I. (2019). Development of recombinant protein-based vaccine against classical swine fever virus in pigs using transgenic nicotiana benthamiana. *Frontiers in Plant Science*, *10*, 624. https://doi.org/10.3389/fpls.2019.00624
17. Stander, J., Chabeda, A., Rybicki, E. P., & Meyers, A. E. (2021). A plant-produced virus-like particle displaying envelope protein domain III elicits an immune response against west nile virus in mice. *Frontiers in Plant Science*, *12*, 738619. https://doi.org/10.3389/fpls.2021.738619
18. Yang, M., Sun, H., Lai, H., Hurtado, J., & Chen, Q. (2018). Plant-produced Zika virus envelope protein elicits neutralizing immune responses that correlate with protective immunity against Zika virus in mice. *Plant Biotechnology Journal*, *16*(2), 572–580. https://doi.org/10.1111/pbi.12796
19. Neuman, B. W., Kiss, G., Kunding, A. H., Bhella, D., Baksh, M. F., Connelly, S., Droese, B., Klaus, J. P., Makino, S., Sawicki, S. G., Siddell, S. G., Stamou, D. G., Wilson, I. A., Kuhn, P., & Buchmeier, M. J. (2011). A structural analysis of M protein in coronavirus assembly and morphology. *Journal of Structural Biology*, *174*(1), 11–22. https://doi.org/10.1016/j.jsb.2010.11.021
20. Ruch, T. R., & Machamer, C. E. (2012). The Coronavirus E protein: Assembly and beyond. *Viruses.*, *4*(3), 363–382. https://doi.org/10.3390/v4030363
21. Thomas, S. (2020). The structure of the membrane protein of SARS-CoV-2 resembles the sugar transporter semiSWEET. *Pathogens and Immunity*, *5*(1), 342. https://doi.org/10.20411/pai.v5i1.377
22. Hassan, Sk. S., Choudhury, P. P., & Roy, B. (2020). SARS-CoV2 envelope protein: Non-synonymous mutations and its consequences. *Genomics*, *112*(6), 3890–3892. https://doi.org/10.1016/j.ygeno.2020.07.001
23. Aldaais, E. A., Yegnaswamy, S., Albahrani, F., Alsowaiket, F., & Alramadan, S. (2021). Sequence and structural analysis of COVID-19 E and M proteins with MERS virus E and M proteins—A comparative study. *Biochemistry and Biophysics Reports*, *26*, 101023. https://doi.org/10.1016/j.bbrep.2021.101023
24. Bianchi, M., Benvenuto, D., Giovanetti, M., Angeletti, S., Ciccozzi, M., & Pascarella, S. (2020). Sars-CoV-2 envelope and membrane proteins: Structural differences linked to virus characteristics? *BioMed Research International*, *2020*, 1–6. https://doi.org/10.1155/2020/4389089
25. Mahtarin, R., Islam, S., Islam, M. J., Ullah, M. O., Ali, M. A., & Halim, M. A. (2022). Structure and dynamics of membrane protein in SARS-CoV-2. *Journal of Biomolecular Structure & Dynamics*, *40*(10), 4725–4738. https://doi.org/10.1080/07391102.2020.1861983
26. Capell, T., Twyman, R. M., Armario-Najera, V., Ma, J. K., Schillberg, S., & Christou, P. (2020). Potential applications of plant biotechnology against SARS-CoV-2. *Trends in Plant Science*, *25*(7), 635–643. https://doi.org/10.1016/j.tplants.2020.04.009
27. Kumar, M., Kumari, N., Thakur, N., Bhatia, S. K., Saratale, G. D., Ghodake, G., Mistry, B. M., Alavilli, H., Kishor, D. S., Du, X., & Chung, S.-M. (2021). A Comprehensive overview on the production of vaccines in plant-based expression systems and the scope of plant biotechnology to combat against SARS-CoV-2 Virus Pandemics. *Plants*, *10*(6), 1213. https://doi.org/10.3390/plants10061213
28. Maharjan, P. M., & Choe, S. (2021). Plant-based COVID-19 vaccines: Current status, design, and development strategies of candidate vaccines. *Vaccines*, *9*(9), 992. https://doi.org/10.3390/vaccines9090992
29. Makatsa, M. S., Tincho, M. B., Wendoh, J. M., Ismail, S. D., Nesamari, R., Pera, F., De Beer, S., David, A., Jugwanth, S., Gededzha, M. P., Mampeule, N., Sanne, I., Stevens, W., Scott, L., Blackburn, J., Mayne, E. S., Keeton, R. S., & Burgers, W. A. (2021). SARS-CoV-2 antigens expressed in plants detect antibody responses in COVID-19 patients. *Frontiers in Plant Science*, *12*, 589940. https://doi.org/10.3389/fpls.2021.589940
30. Pogrebnyak, N., Golovkin, M., Andrianov, V., Spitsin, S., Smirnov, Y., Egolf, R., & Koprowski, H. (2005). Severe acute respiratory syndrome (SARS) S protein production in plants: Development of recombinant vaccine. *The Proceedings of the National Academy of Sciences*, *102*(25), 9062–9067. https://doi.org/10.1073/pnas.0503760102
31. Jung, J., Zahmanova, G., Minkov, I., & Lomonossoff, G. P. (2022). Plant-based expression and characterization of SARS-CoV-2 virus-like particles presenting a native spike protein. *Plant Biotechnology Journal*, *20*(7), 1363–1372. https://doi.org/10.1111/pbi.13813
32. Moon, K.-B., Jeon, J.-H., Choi, H., Park, J.-S., Park, S.-J., Lee, H.-J., Park, J. M., Cho, H. S., Moon, J. S., Oh, H., Kang, S., Mason, H. S., Kwon, S.-Y., & Kim, H.-S. (2022). Construction of SARS-CoV-2 virus-like particles in plant. *Scientific Reports*, *12*(1), 1005. https://doi.org/10.1038/s41598-022-04883-y
33. Ward, B. J., Gobeil, P., Séguin, A., Atkins, J., Boulay, I., Charbonneau, P.-Y., Couture, M., D'Aoust, M.-A., Dhaliwall, J., Finkle, C., Hager, K., Mahmood, A., Makarkov, A., Cheng, M. P., Pillet, S., Schimke, P., St-Martin, S., Trépanier, S., & Landry, N. (2021). Phase 1 randomized trial of a plant-derived virus-like particle vaccine for COVID-19. *Nature Medicine*, *27*(6), 1071–1078. https://doi.org/10.1038/s41591-021-01370-1
34. Rattanapisit, K., Shanmugaraj, B., Manopwisedjaroen, S., Purwono, P. B., Siriwattananon, K., Khorattanakulchai, N., Hanittinan, O., Boonyayothin, W., Thitithanyanont, A., Smith, D. R., & Phoolcharoen, W. (2020). Rapid production of SARS-CoV-2 receptor binding domain (RBD) and spike specific monoclonal antibody CR3022 in Nicotiana benthamiana. *Scientific Reports*, *10*(1), 17698. https://doi.org/10.1038/s41598-020-74904-1
35. McLean, G., Kamil, J., Lee, B., Moore, P., Schulz, T. F., Muik, A., Sahin, U., Türeci, Ö., & Pather, S. (2022). The impact of evolving SARS-CoV-2 mutations and variants on COVID-19 vaccines. *MBio*, *13*(2), e02979–21. https://doi.org/10.1128/mbio.02979-21
36. Mohammad, T., Choudhury, A., Habib, I., Asrani, P., Mathur, Y., Umair, M., Anjum, F., Shafie, A., Yadav, D. K., & Hassan, Md. I. (2021). Genomic variations in the structural proteins of SARS-CoV-2 and their

deleterious impact on pathogenesis: A comparative genomics approach comparative genomics approach. *Frontiers in Cellular and Infection Microbiology*, *11*, 765039. https://doi.org/10.3389/fcimb.2021.765039
37. Shen, L., Bard, J. D., Triche, T. J., Judkins, A. R., Biegel, J. A., & Gai, X. (2021). Emerging variants of concern in SARS-CoV-2 membrane protein: A highly conserved target with potential pathological and therapeutic implications. *Emerging Microbes & Infections*, *10*(1), 885–893. https://doi.org/10.1080/22221751.2021.1922097
38. Jörrißen, P., Schütz, P., Weiand, M., Vollenberg, R., Schrempf, I. M., Ochs, K., Frömmel, C., Tepasse, P.-R., Schmidt, H., & Zibert, A. (2021). Antibody response to SARS-CoV-2 membrane protein in patients of the acute and convalescent phase of COVID-19. *Frontiers in Immunology*, *12*, 679841. https://doi.org/10.3389/fimmu.2021.679841
39. Smits, V. A. J., Hernández-Carralero, E., Paz-Cabrera, M. C., Cabrera, E., Hernández-Reyes, Y., Hernández-Fernaud, J. R., Gillespie, D. A., Salido, E., Hernández-Porto, M., & Freire, R. (2021). The Nucleocapsid protein triggers the main humoral immune response in COVID-19 patients. *Biochemical and Biophysical Research Communications*, *543*, 45–49. https://doi.org/10.1016/j.bbrc.2021.01.073
40. Sarrion-Perdigones, A., Vazquez-Vilar, M., Palaci, J., Castelijns, B., Forment, J., Ziarsolo, P., Blanca, J., Granell, A., & Orzaez, D. (2013). GoldenBraid 2.0: A comprehensive DNA assembly framework for plant synthetic biology. *Plant Physiology*, *162*(3), 1618–1631. https://doi.org/10.1104/pp.113.217661
41. Sarrion-Perdigones, A., Palaci, J., Granell, A., & Orzaez, D. (2014). Design and construction of multigenic constructs for plant biotechnology using the goldenbraid cloning strategy. In S. Valla, & R. Lale (Eds.), *DNA cloning and assembly methods* (Vol. 1116, pp. 133–151). Humana Press. https://doi.org/10.1007/978-1-62703-764-8_10
42. Gunadi, A., Rushton, P. J., McHale, L. K., Gutek, A. H., & Finer, J. J. (2016). Characterization of 40 soybean (Glycine max) promoters, isolated from across 5 thematic gene groups. *Plant Cell, Tissue and Organ Culture (PCTOC)*, *127*(1), 145–160. https://doi.org/10.1007/s11240-016-1038-x
43. Norris, S. R., Meyer, S. E., & Callis, J. (1993). The intron of Arabidopsis thaliana polyubiquitin genes is conserved in location and is a quantitative determinant of chimeric gene expression. *Plant Molecular Biology*, *21*(5), 895–906. https://doi.org/10.1007/BF00027120
44. Cai, Y., McClinchie, E., Price, A., Nguyen, T. N., Gidda, S. K., Watt, S. C., Yurchenko, O., Park, S., Sturtevant, D., Mullen, R. T., Dyer, J. M., & Chapman, K. D. (2017). Mouse fat storage-inducing transmembrane protein 2 (FIT 2) promotes lipid droplet accumulation in plants. *Plant Biotechnology Journal*, *15*(7), 824–836. https://doi.org/10.1111/pbi.12678
45. Vanhercke, T., El Tahchy, A., Liu, Q., Zhou, X., Shrestha, P., Divi, U. K., Ral, J., Mansour, M. P., Nichols, P. D., James, C. N., Horn, P. J., Chapman, K. D., Beaudoin, F., Ruiz-López, N., Larkin, P. J., Feyter, R. C., Singh, S. P., & Petrie, J. R. (2014). Metabolic engineering of biomass for high energy density: Oilseed-like triacylglycerol yields from plant leaves. *Plant Biotechnology Journal*, *12*(2), 231–239. https://doi.org/10.1111/pbi.12131
46. Mirdita, M., Schütze, K., Moriwaki, Y., Heo, L., Ovchinnikov, S., & Steinegger, M. (2022). ColabFold: Making protein folding accessible to all. *Nature Methods*, *19*(6), 679–682. https://doi.org/10.1038/s41592-022-01488-1
47. Hager, K. J., Pérez Marc, G., Gobeil, P., Diaz, R. S., Heizer, G., Llapur, C., Makarkov, A. I., Vasconcellos, E., Pillet, S., Riera, F., Saxena, P., Geller Wolff, P., Bhutada, K., Wallace, G., Aazami, H., Jones, C. E., Polack, F. P., Ferrara, L., Atkins, J., … Ward, B. J. (2022). Efficacy and safety of a recombinant plant-based adjuvanted Covid-19 vaccine. *New England Journal of Medicine*, *386*(22), 2084–2096. https://doi.org/10.1056/NEJMoa2201300
48. Müntz, K. (1998). *Plant Molecular Biology*, *38*(1/2), 77–99. https://doi.org/10.1023/A:1006020208380
49. Lau, O. S., & Sun, S. S. M. (2009). Plant seeds as bioreactors for recombinant protein production. *Biotechnology Advances*, *27*(6), 1015–1022. https://doi.org/10.1016/j.biotechadv.2009.05.005
50. Jolivet, P., Roux, E., D'Andrea, S., Davanture, M., Negroni, L., Zivy, M., & Chardot, T. (2004). Protein composition of oil bodies in Arabidopsis thaliana ecotype WS. *Plant Physiology and Biochemistry*, *42*(6), 501–509.
51. Jolivet, P., Tailliart, K., Boulard, C., Nesi, N., & Chardot, T. (2006). Purification and protein composition of oil bodies from Brassica napus seeds. *Operations Control Language*, *13*(6), 426–430.
52. Marion, J., Bach, L., Bellec, Y., Meyer, C., Gissot, L., & Faure, J. D. (2008). Systematic analysis of protein subcellular localization and interaction using high-throughput transient transformation of Arabidopsis seedlings. *Plant Journal*, *56*(1), 169–179. https://doi.org/10.1111/j.1365-313X.2008.03596.x
53. Gräwe, A., Ranglack, J., Weyrich, A., & Stein, V. (2020). iFLinkC: An iterative functional linker cloning strategy for the combinatorial assembly and recombination of linker peptides with functional domains. *Nucleic acids research*, *48*(4), e24–. https://doi.org/10.1093/nar/gkz1210
54. Prasad, V., & Bartenschlager, R. (2023). A snapshot of protein trafficking in SARS-CoV-2 infection. *Biology of the Cell*, *115*(2), 2200073. https://doi.org/10.1111/boc.202200073
55. Yokomori, H., Ando, W., & Oda, M. (2019). Caveolin-1 is related to lipid droplet formation in hepatic stellate cells in human liver. *Acta Histochemica*, *121*(2), 113–118. https://doi.org/10.1016/j.acthis.2018.10.008
56. Renard, H. F., Demaegd, D., Guerriat, B., & Morsomme, P. (2010). Efficient ER exit and vacuole targeting of yeast Sna2p require two tyrosine-based sorting motifs. *Traffic (Copenhagen, Denmark)*, *11*(7), 931–946.
57. Miyanari, Y., Atsuzawa, K., Usuda, N., Watashi, K., Hishiki, T., Zayas, M., Bartenschlager, R., Wakita, T., Hijikata, M., & Shimotohno, K. (2007). The lipid droplet is an important organelle for hepatitis C virus production. *Nature Cell Biology*, *9*(9), 1089–1097. https://doi.org/10.1038/ncb1631
58. Dias, S. S. G., Soares, V. C., Ferreira, A. C., Sacramento, C. Q., Fintelman-Rodrigues, N., Temerozo, J. R., Teixeira, L., Nunes Da Silva, M. A., Barreto, E., Mattos, M., De Freitas, C. S., Azevedo-Quintanilha, I. G., Manso, P. P. A., Miranda, M. D., Siqueira, M. M., Hottz, E. D., Pão, C. R. R., Bou-Habib, D. C., Barreto-Vieira, D. F., … Bozza, P. T. (2020). Lipid droplets fuel SARS-CoV-2 replication and production of inflammatory mediators. *Plos Pathogens*, *16*(12), e1009127. https://doi.org/10.1371/journal.ppat.1009127
59. Grootemaat, A. E., Van Der Niet, S., Scholl, E. R., Roos, E., Schurink, B., Bugiani, M., Miller, S. E., Larsen, P., Pankras, J., Reits, E. A., & Van Der Wel, N. N. (2022). Lipid and nucleocapsid N-protein accumulation in COVID-19 patient lung and infected cells patient lung and infected cells. *Microbiology Spectrum*, *10*(1), e01271–21. https://doi.org/10.1128/spectrum.01271-21
60. Morineau, C., Bellec, Y., Tellier, F., Gissot, L., Kelemen, Z., Nogue, F., & Faure, J.-D. (2017). Selective gene dosage by CRISPR -Cas9 genome editing in hexaploid Camelina sativa. *Plant Biotechnology Journal*, *15*(6), 729–739. https://doi.org/10.1111/pbi.12671
61. Morineau, C., Gissot, L., Bellec, Y., Hematy, K., Tellier, F., Renne, C., Haslam, R., Beaudoin, F., Napier, J., & Faure, J.-D. (2016). Dual fatty acid elongase complex interactions in arabidopsis. *PLoS ONE*, *11*(9), e0160631. https://doi.org/10.1371/journal.pone.0160631
62. Adler, J., & Parmryd, I. (2010). Quantifying colocalization by correlation: The Pearson correlation coefficient is superior to the Mander's overlap coefficient. *Cytometry, Part A*, *77A*(8), 733–742. https://doi.org/10.1002/cyto.a.20896
63. Deruyffelaere, C., Bouchez, I., Morin, H., Guillot, A., Miquel, M., Froissard, M., Chardot, T., & D'Andrea, S. (2015). Ubiquitin-mediated proteasomal degradation of oleosins is involved in oil body mobiliza-

tion during post-germinative seedling growth in arabidopsis. *Plant & Cell Physiology*, https://doi.org/10.1093/pcp/pcv056

64. D'Andrea, S., Jolivet, P., Boulard, C., Larre, C., Froissard, M., & Chardot, T. (2007). Selective one-step extraction of arabidopsis thaliana seed oleosins using organic solvents. *Journal of Agricultural and Food Chemistry*, *55*(24), 10008–10015.

SUPPORTING INFORMATION

Additional supporting information can be found online in the Supporting Information section at the end of this article.

How to cite this article: Gissot, L., Fontaine, F., Kelemen, Z., Dao, O., Bouchez, I., Deruyffelaere, C., Winkler, M., Costa, A. D., Pierre, F., Meziadi, C., Faure, J.-D., & Froissard, M. (2024). E and M SARS-CoV-2 membrane protein expression and enrichment with plant lipid droplets. *Biotechnology Journal*, *19*, e2300512. https://doi.org/10.1002/biot.202300512